Electronic Supporting Information

Synthesis, characterization and catecholase activity of dinuclear cobalt (II/III) complexes of a o-donor rich Schiff base ligand

Suman Kr Dey and Arindam Mukherjee*

Contents

Table S1 Selected bond distances (Å) and angles (deg) for **1-3**.

1		**2**		**3**	
Co(1)…Co(1)#1	2.8640(16)	Co(1)…Co(2)	3.005(1)	Co(1)…Co(2)	2.9961(7)
Co(1)-O(4)	1.862(3)	Co(1)-O(1)	1.896(5)	Co(1)-O(1)	1.876(3)
Co(1)-N(1)	1.869(4)	Co(1)-O(2)	1.916(5)	Co(1)-O(5)	1.883(3)
Co(1)-O(1)	1.912(3)	Co(1)-O(5)	1.894(5)	Co(1)-N(2)	1.903(3)
Co(1)-O(1)#1	1.918(3)	Co(1)-O(6)	1.942(5)	Co(1)-N(1)	1.905(3)
Co(1)-O(2)	1.945(3)	Co(1)-N(1)	1.912(6)	Co(1)-O(2)	1.917(3)
Co(1)-O(5)	1.948(3)	Co(1)-N(2)	1.908(6)	Co(1)-O(6)	1.927(2)
O(1)-Co(1)#1	1.918(3)	Co(2)-O(2)	2.042(5)	Co(2)-O(2)	2.028(3)
		Co(2)-O(3)	2.056(5)	Co(2)-O(6)	2.047(3)
O(4)-Co(1)-N(1)	95.72(14)	Co(2)-O(6)	2.037(5)	Co(2)-O(7)	2.059(3)
O(4)-Co(1)-O(1)	93.27(12)	Co(2)-O(7)	2.085(5)	Co(2)-O(9)	2.096(3)
N(1)-Co(1)-O(1)	87.32(13)	Co(2)-O(9)	2.190(5)	Co(2)-O(3)	2.096(3)
O(4)-Co(1)-O(1)#1	176.37(13)	Co(2)-O(10)	2.147(5)	Co(2)-N(3)	2.127(3)
N(1)-Co(1)-O(1)#1	85.10(13)				
O(1)-Co(1)-O(1)#1	83.23(13)	O(5)-Co(1)-O(2)	92.6(2)	O(1)-Co(1)-O(5)	90.88(12)
O(4)-Co(1)-O(2)	90.02(13)	O(5)-Co(1)-O(6)	176.5(2)	O(1)-Co(1)-N(2)	88.58(12)
N(1)-Co(1)-O(2)	173.71(14)	O(5)-Co(1)-O(1)	91.6(2)	O(5)-Co(1)-N(2)	95.00(12)
O(1)-Co(1)-O(2)	94.95(12)	O(5)-Co(1)-N(2)	95.1(2)	O(1)-Co(1)-N(1)	95.38(12)
O(1)#1-Co(1)-O(2)	89.34(12)	O(5)-Co(1)-N(1)	88.1(2)	O(5)-Co(1)-N(1)	87.69(11)
O(4)-Co(1)-O(5)	91.36(13)	O(2)-Co(1)-O(6)	84.3(2)	N(2)-Co(1)-N(1)	175.18(12)
N(1)-Co(1)-O(5)	89.67(14)	O(1)-Co(1)-O(2)	175.7(2)	O(1)-Co(1)-O(2)	177.16(11)
O(1)-Co(1)-O(5)	174.70(12)	O(1)-Co(1)-O(6)	91.5(2)	O(5)-Co(1)-O(2)	91.87(11)
O(1)#1-Co(1)-O(5)	92.17(12)	O(1)-Co(1)-N(2)	87.6(2)	N(2)-Co(1)-O(2)	91.89(11)
O(2)-Co(1)-O(5)	87.61(12)	O(1)-Co(1)-N(1)	94.8(2)	N(1)-Co(1)-O(2)	84.01(11)
Co(1)-O(1)-Co(1)#1	96.77(13)	N(2)-Co(1)-O(2)	93.0(2)	O(1)-Co(1)-O(6)	92.65(11)
		N(2)-Co(1)-O(6)	83.4(2)	O(5)-Co(1)-O(6)	176.43(11)
		N(2)-Co(1)-N(1)	176.0(3)	N(2)-Co(1)-O(6)	84.56(11)
		N(1)-Co(1)-O(2)	84.4(2)	N(1)-Co(1)-O(6)	92.51(11)
		N(1)-Co(1)-O(6)	93.3(2)	O(2)-Co(1)-O(6)	84.60(11)
		O(2)-Co(2)-O(9)	166.65(19)	O(2)-Co(2)-O(6)	78.81(10)
		O(2)-Co(2)-O(10)	106.2(2)	O(2)-Co(2)-O(7)	92.48(11)
		O(2)-Co(2)-O(7)	94.0(2)	O(6)-Co(2)-O(7)	91.13(11)
		O(2)-Co(2)-O(3)	92.6(2)	O(2)-Co(2)-O(9)	172.82(11)
		O(10)-Co(2)-O(9)	60.45(19)	O(6)-Co(2)-O(9)	94.20(11)
		O(6)-Co(2)-O(9)	114.50(19)	O(7)-Co(2)-O(9)	89.29(12)
		O(6)-Co(2)-O(2)	78.8(2)	O(2)-Co(2)-O(3)	90.13(10)
		O(6)-Co(2)-O(10)	174.1(2)	O(6)-Co(2)-O(3)	89.71(10)
		O(6)-Co(2)-O(7)	90.1(2)	O(7)-Co(2)-O(3)	177.37(12)
		O(6)-Co(2)-O(3)	88.2(2)	O(9)-Co(2)-O(3)	88.16(11)
		O(7)-Co(2)-O(9)	86.6(2)	O(2)-Co(2)-N(3)	96.74(12)
		O(7)-Co(2)-O(10)	92.7(2)	O(6)-Co(2)-N(3)	174.92(12)
		O(3)-Co(2)-O(9)	87.7(2)	O(7)-Co(2)-N(3)	91.53(13)
		O(3)-Co(2)-O(10)	88.4(2)	O(9)-Co(2)-N(3)	90.16(13)
		O(3)-Co(2)-O(7)	172.7(2)	O(3)-Co(2)-N(3)	87.82(12)
		Co(1)-O(2)-Co(2)	98.8(2)	Co(1)-O(2)-Co(2)	98.77(11)
		Co(1)-O(6)-Co(2)	98.1(2)	Co(1)-O(6)-Co(2)	97.81(11)

Symmetry transformations used to generate equivalent atoms: #1 -x+1,-y,-z+1

Table S2 The bond valence sum calculation for **1-3.**

	1		**2**		**3**	
Co-site	Co(II)	Co(III)	Co(II)	Co(III)	Co(II)	Co(III)
Co(1)	3.49	3.16	3.47	3.13	3.52	3.19
Co(2)	---	---	2.10	1.91	2.19	1.98

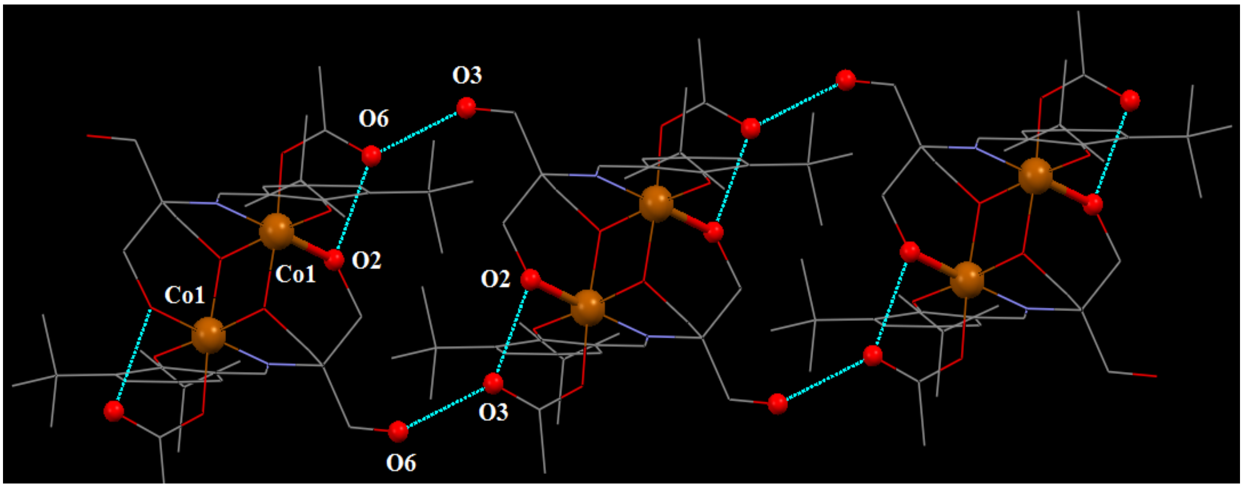

Fig. S1 View of a 1D chain linked by intermolecular hydrogen bonding in Complex **1**. Hydrogen atoms are omitted for clarity.

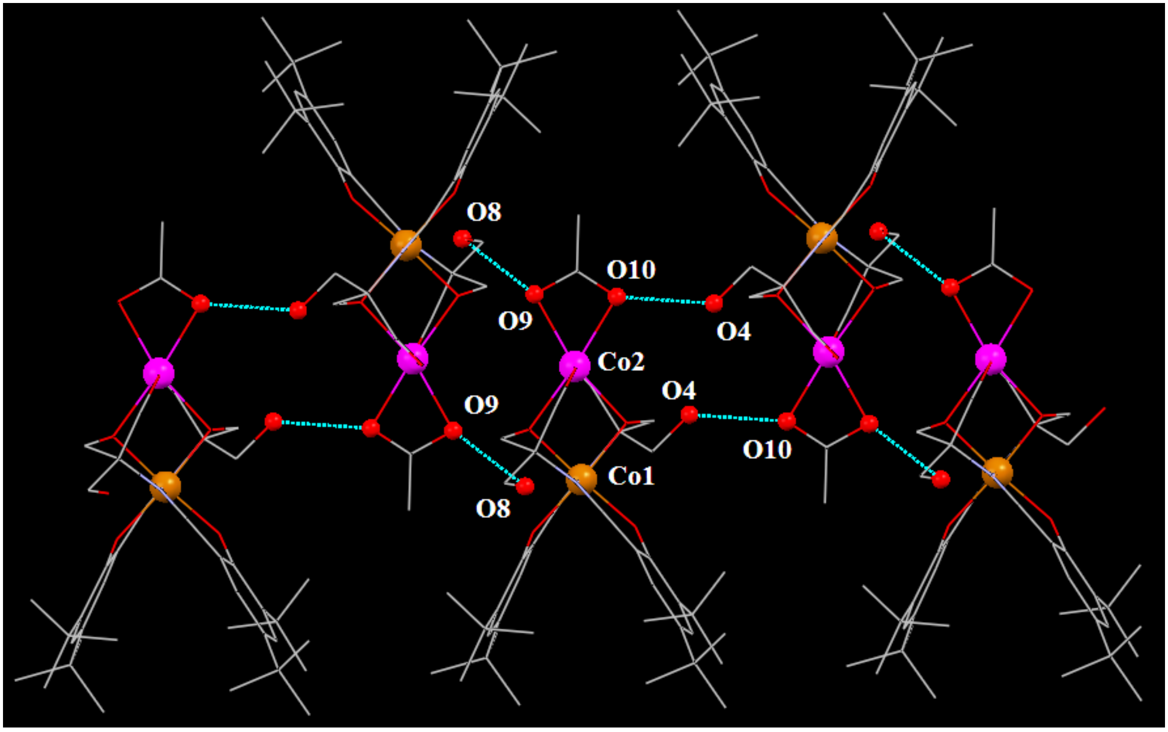

Fig. S2 View of a 1D chain linked by intermolecular hydrogen bonding in Complex **2**. Hydrogen atoms are omitted for clarity.

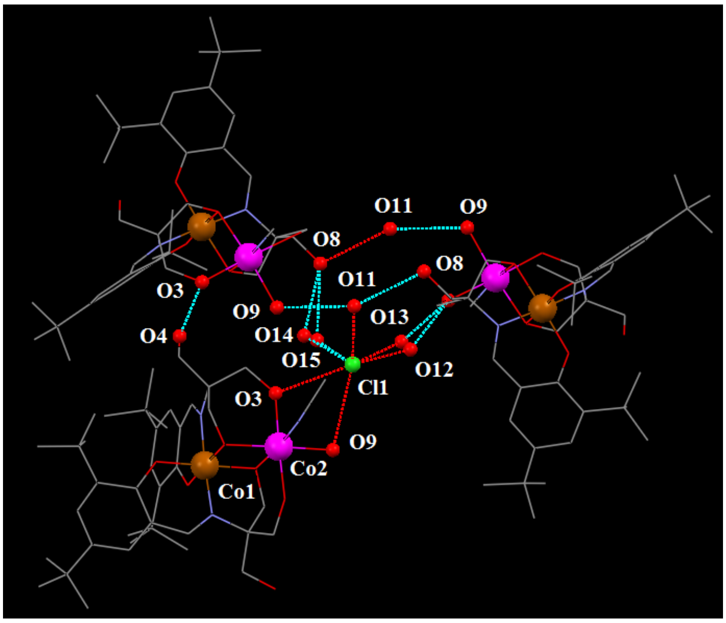

Fig. S3 View of different type of intermolecular hydrogen bonding in Complex **3**. Hydrogen atoms are omitted for clarity. O12, O13 and O14, O15 are two disordered water molecules respectively

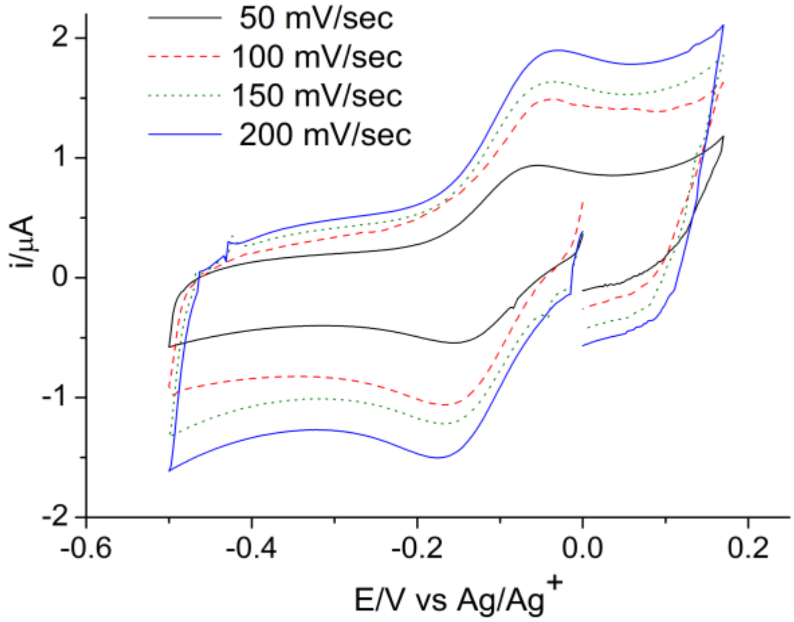

Fig. S4 Cyclic voltammogram of **1** in DMF (showing only Co^{III}/Co^{II} peak) with 0.1 M TBAP as supporting electrolyte. The measurements were conducted using a glassy carbon working electrode at different scan rates as mentioned.

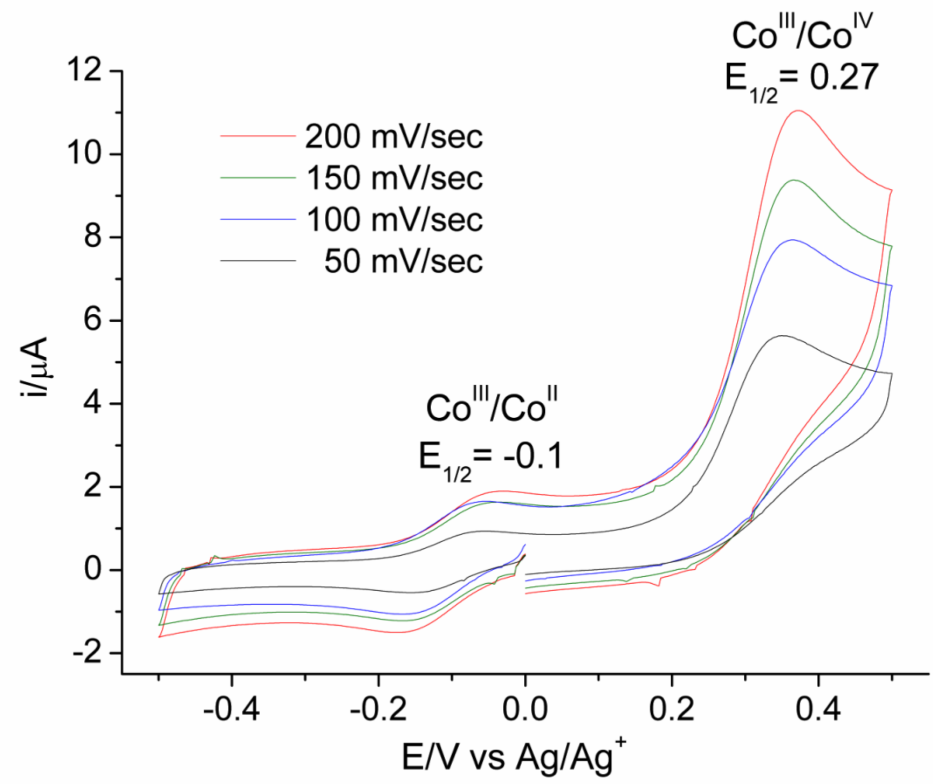

Fig. S5 Cyclic voltammogram of **1** in DMF (showing only the metal centred peaks) with 0.1 M TBAP as supporting electrolyte. The measurements were conducted using a glassy carbon working electrode at different scan rates as mentioned.

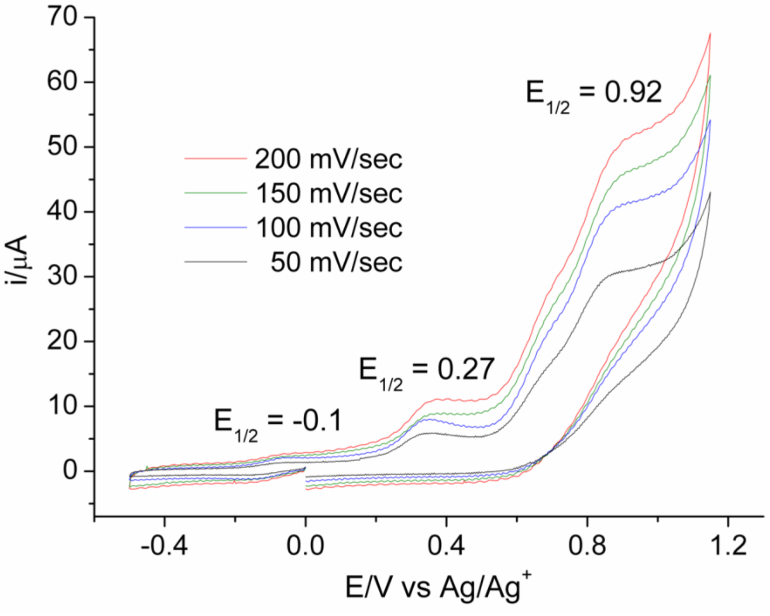

Fig. S6 Cyclic voltammogram of **1** in DMF with 0.1 M TBAP as supporting electrolyte. The measurements were conducted using a glassy carbon working electrode at different scan rates as mentioned.

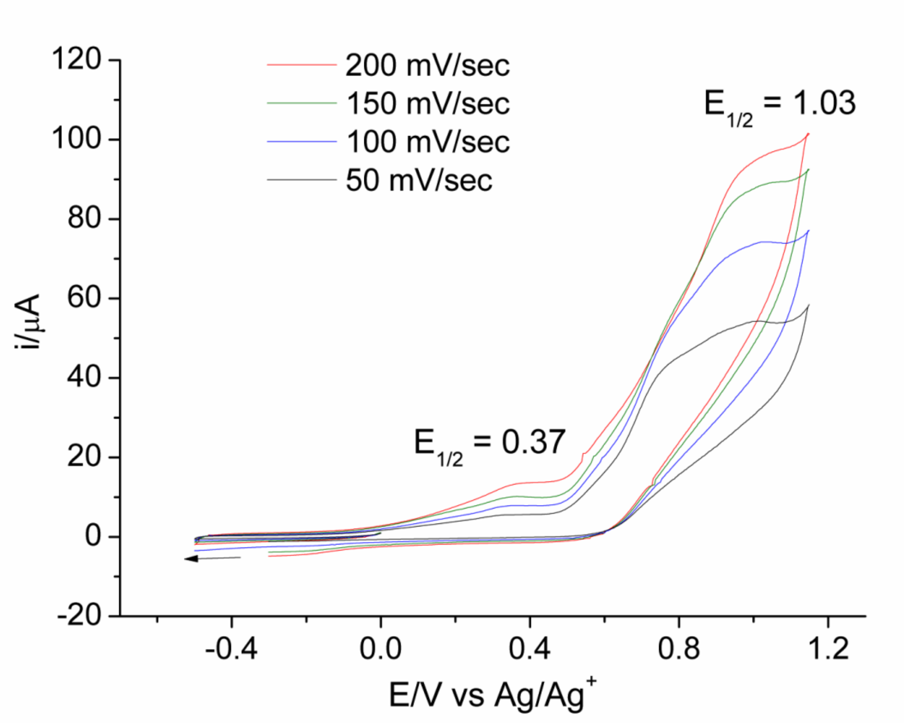

Fig. S7 Cyclic voltammogram of **2** in DMF with 0.1 M TBAP as supporting electrolyte. The measurements were conducted using a glassy carbon working electrode at different scan rates as mentioned.

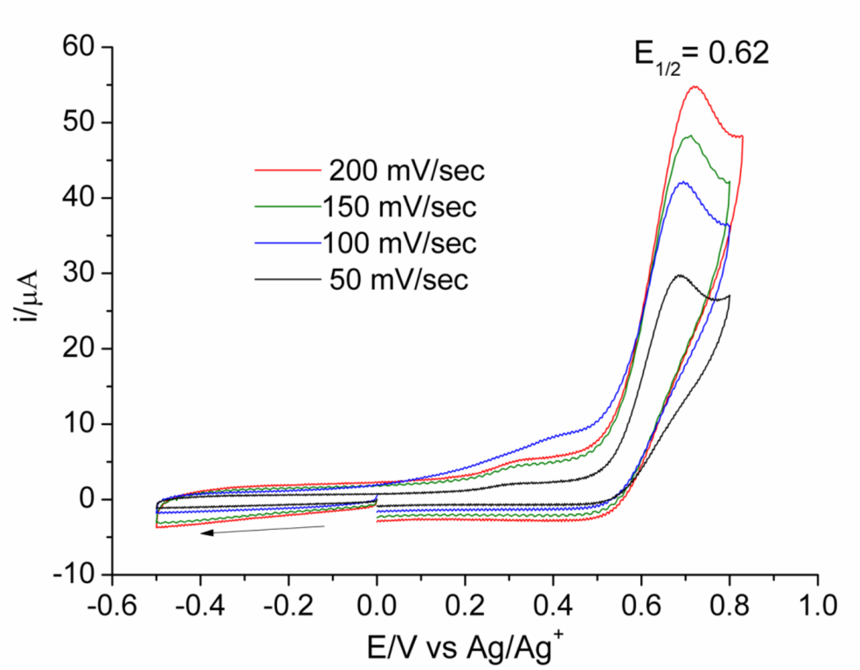

Fig. S8 Cyclic voltammogram of **3** in DMF with 0.1 M TBAP as supporting electrolyte. The measurements were conducted using a glassy carbon working electrode at different scan rates as mentioned.

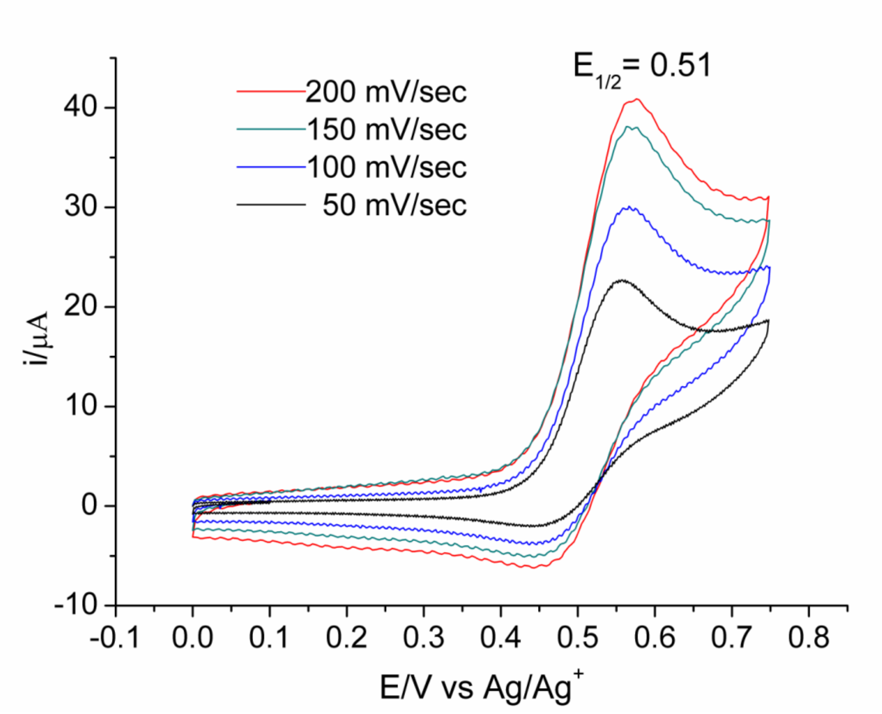

Fig. S9 Cyclic voltammogram of H_4L in DMF with 0.1 M TBAP as supporting electrolyte. The measurements were conducted using a glassy carbon working electrode at different scan rates as mentioned.

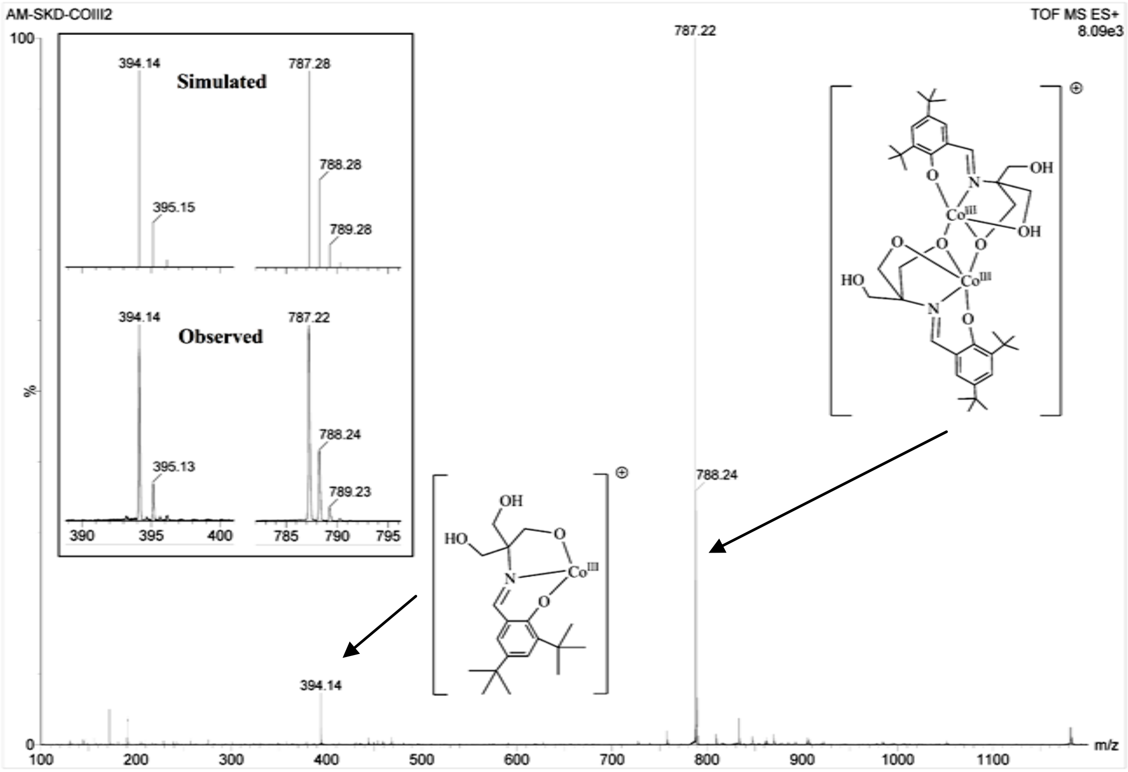

Fig. S10 ESI-MS (+ve ion mode) of complex **1** in (1:1) methanol:acetonitrile with 1% DMF, along with the speciation. Inset shows isotropic distribution of the assigned peaks.

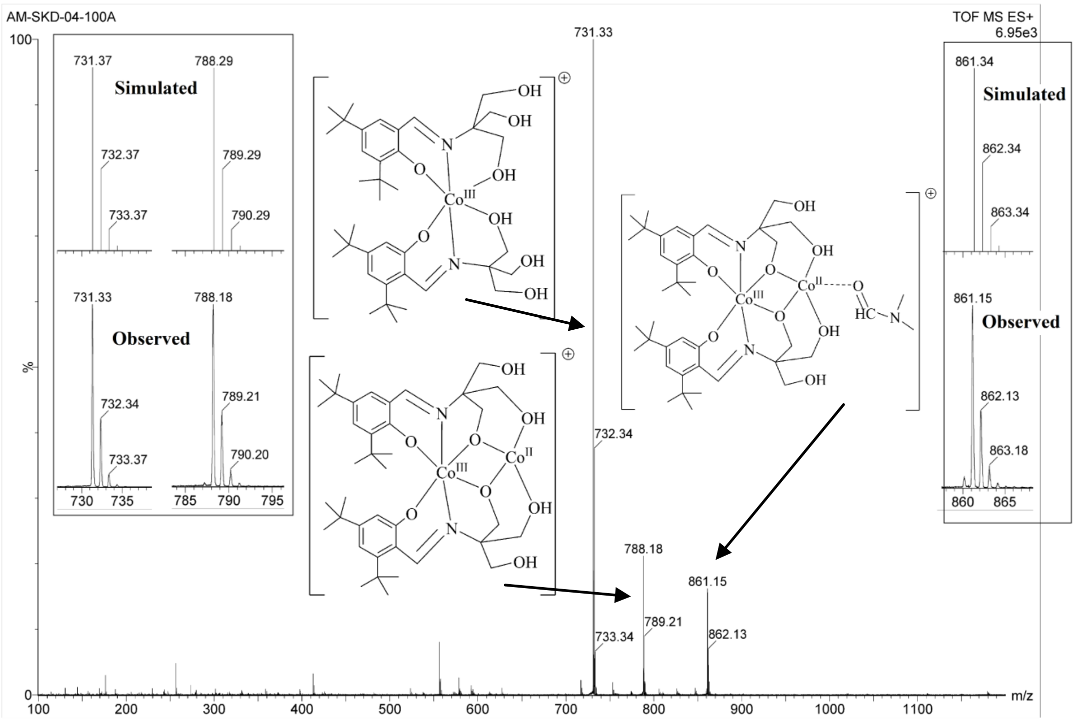

Fig. S11 ESI-MS (+ve ion mode) of complex **2** in (1:1) methanol:acetonitrile with 1% DMF, along with the speciation. Insets show isotropic distribution of the assigned peaks.

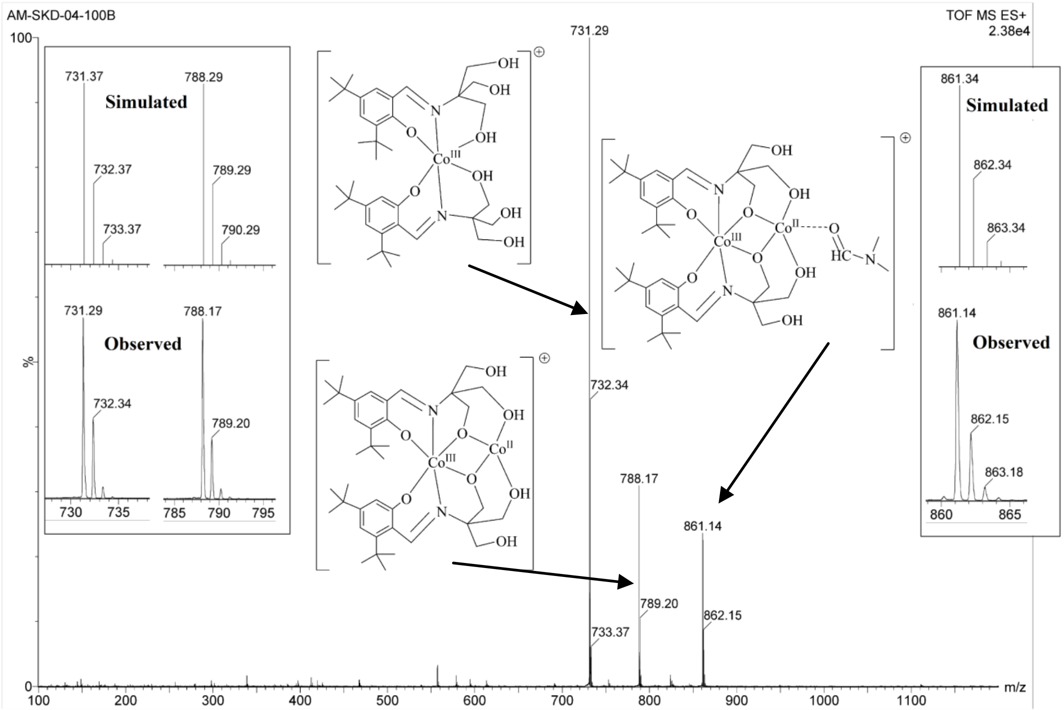

Fig. S12 ESI-MS (+ve ion mode) of complex **3** in (1:1) methanol:acetonitrile with 1% DMF, along with the speciation. Insets show isotropic distribution of the assigned peaks.

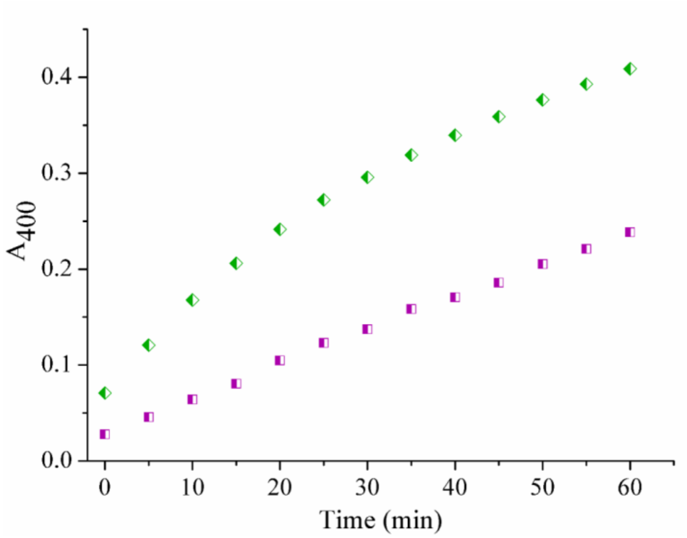

Fig. S13 Inhibition study of catechol oxidation by probucol probed for an hour by monitoring the change in absorbance at 400 nm using 500 molar equivalents of DTBC and 0.1 μM of **1** without probucol (green) and with 40 molar equivalent probucol (purple).

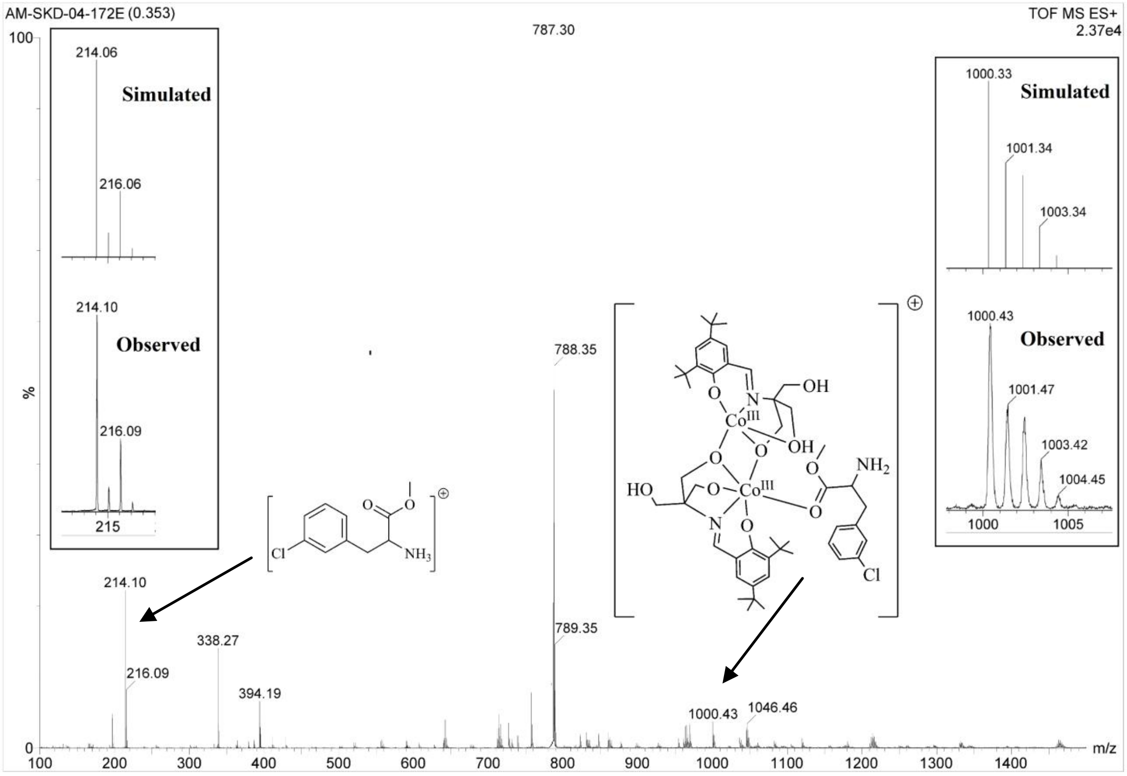

Fig. S14 ESI-MS (+ve ion mode) of the mixture of methyl ester of *p*-chlorophenylalanine with complex **1** in (1:1) methanol:acetonitrile with 1% DMF. Reaction condition: 10 μM catalyst (**1**) in air with 3 molar equivalents of methyl ester of *p*-chlorophenylalanine. Insets show isotropic distribution of the assigned peaks.

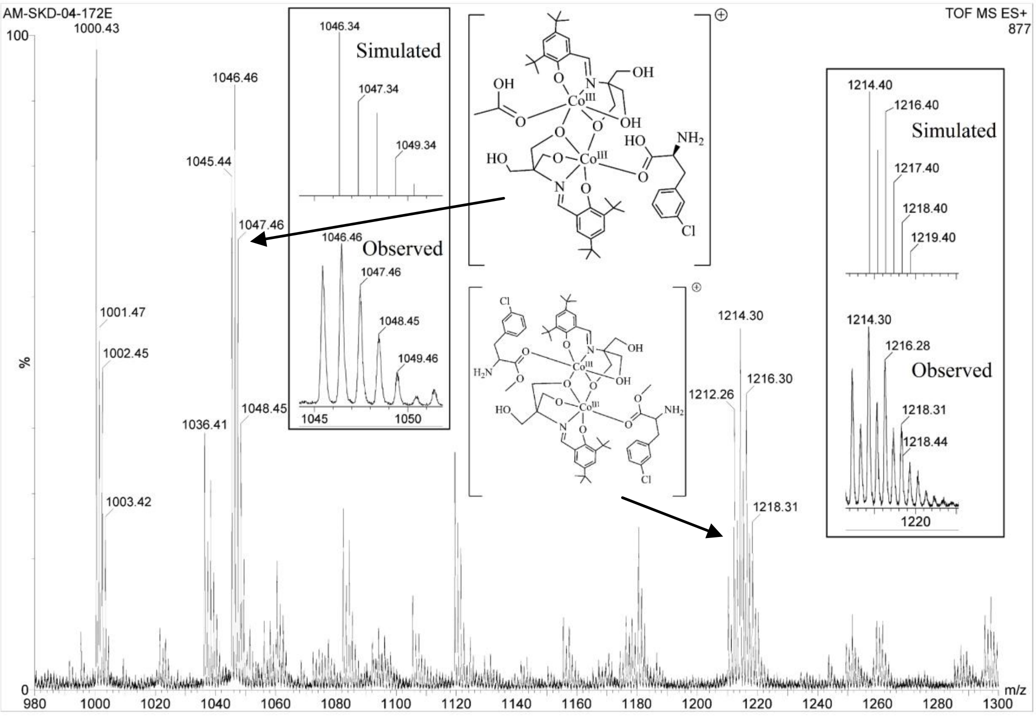

Fig. S15 ESI-MS (+ve ion mode) of the mixture of methyl ester of *p*-chlorophenylalanine with complex **1** in (1:1) methanol:acetonitrile with 1% DMF. (showing m/z from 980 to 1300). Insets show isotropic distribution of the assigned peaks.

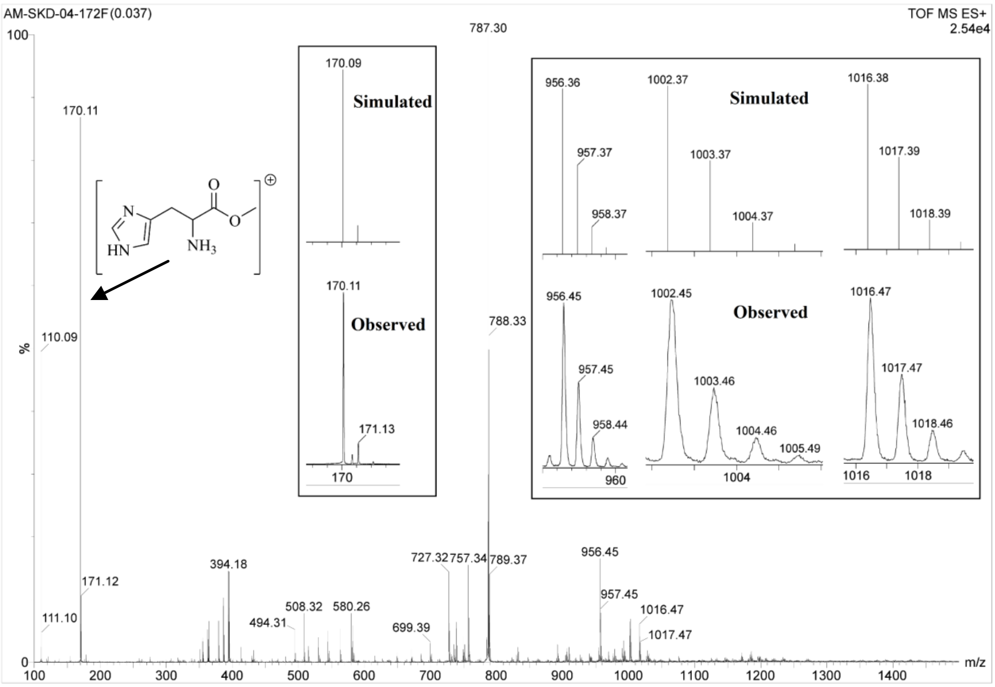

Fig. S16 ESI-MS (+ve ion mode) of the mixture of methyl ester of histidine with complex **1** in (1:1) methanol:acetonitrile with 1% DMF. Reaction condition: 10 μM catalyst (**1**) in air with 3 molar equivalents of methyl ester of histidine. Insets show isotropic distribution of the assigned peaks.

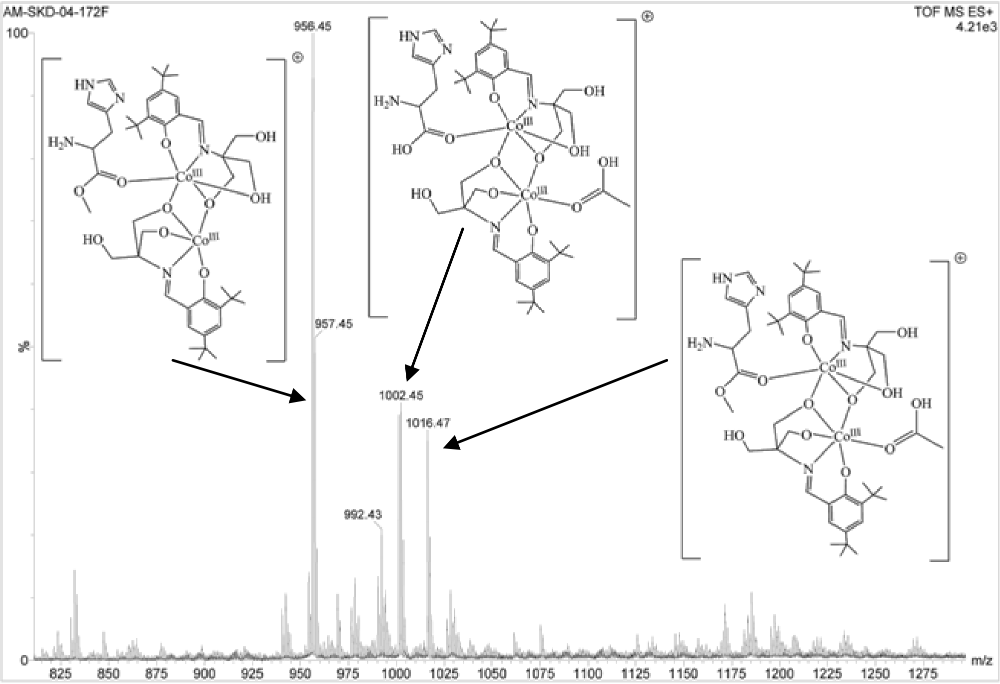

Fig. S17 ESI-MS (+ve ion mode) of the mixture of methyl ester of histidine with complex **1** in (1:1) methanol:acetonitrile with 1% DMF. Reaction condition: 10 μM catalyst (**1**) in air with 3 molar equivalents of methyl ester of histidine (showing m/z from 800 to 1300).

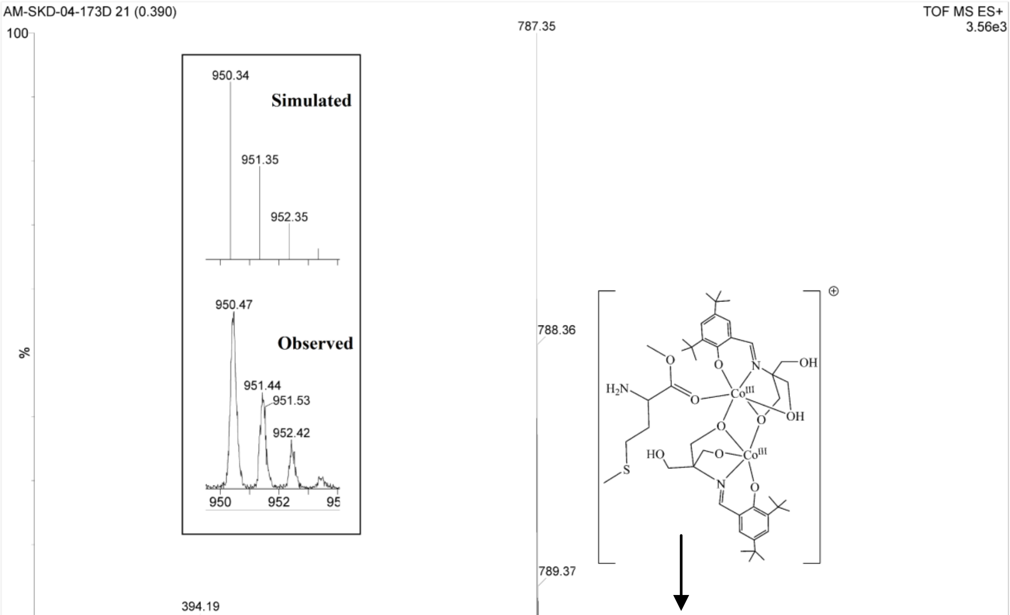

Fig. S18 ESI-MS (+ve ion mode) of the mixture of methyl ester of methionine with complex **1** in (1:1) methanol:acetonitrile with 1% DMF. Reaction condition: 10 μM catalyst (**1**) in air with 3 molar equivalents of methyl ester of methionine. Insets show isotropic distribution of the assigned peaks.

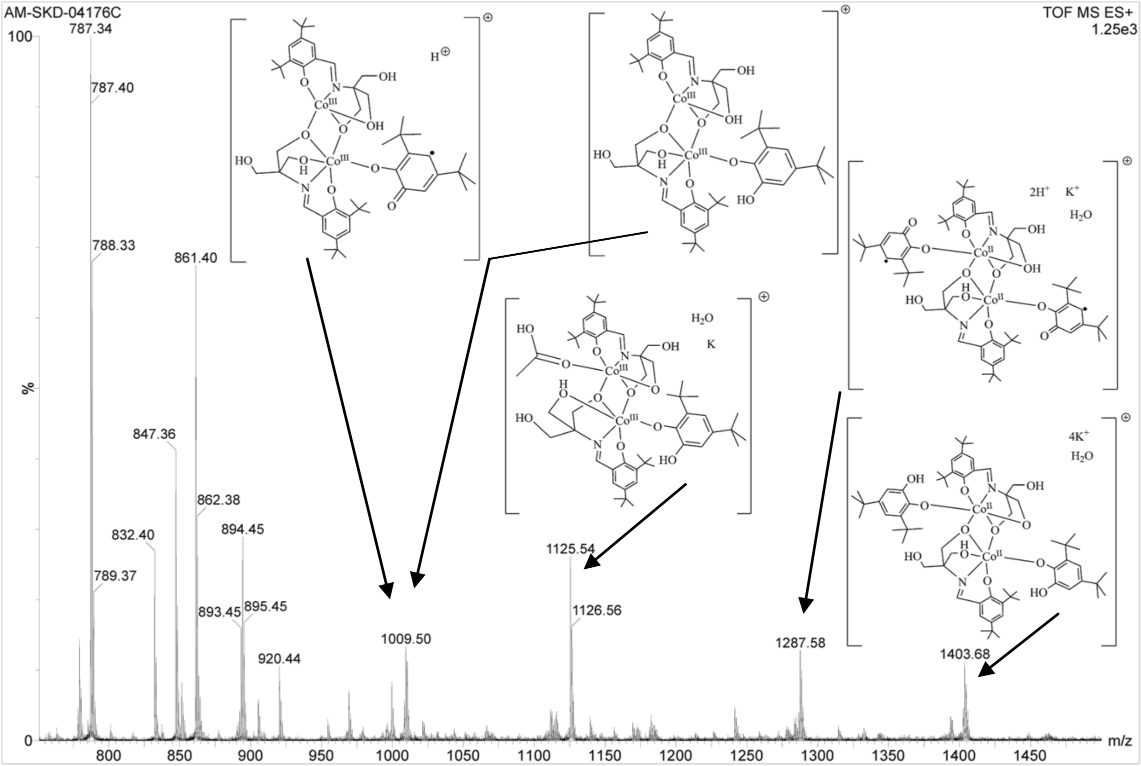

Fig. S19A ESI-MS (+ve ion mode) of the mixture of DTBC with complex **1** in (1:1) methanol:acetonitrile with 1% DMF, along with the speciation. Reaction condition: 10 μM catalyst (**1**) in air with 500 molar equivalents of DTBC.

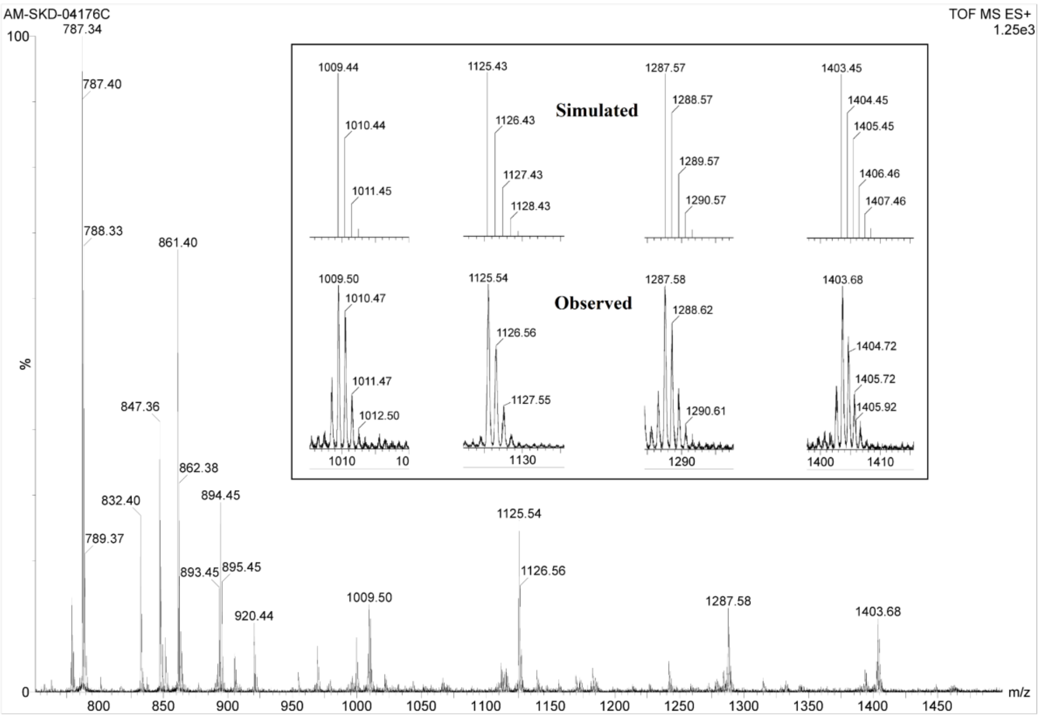

Fig. S19B ESI-MS (+ve ion mode) of the mixture of DTBC with complex **1** in (1:1) methanol:acetonitrile with 1% DMF, with isotopic distribution of the peaks assigned in Fig. S19A.

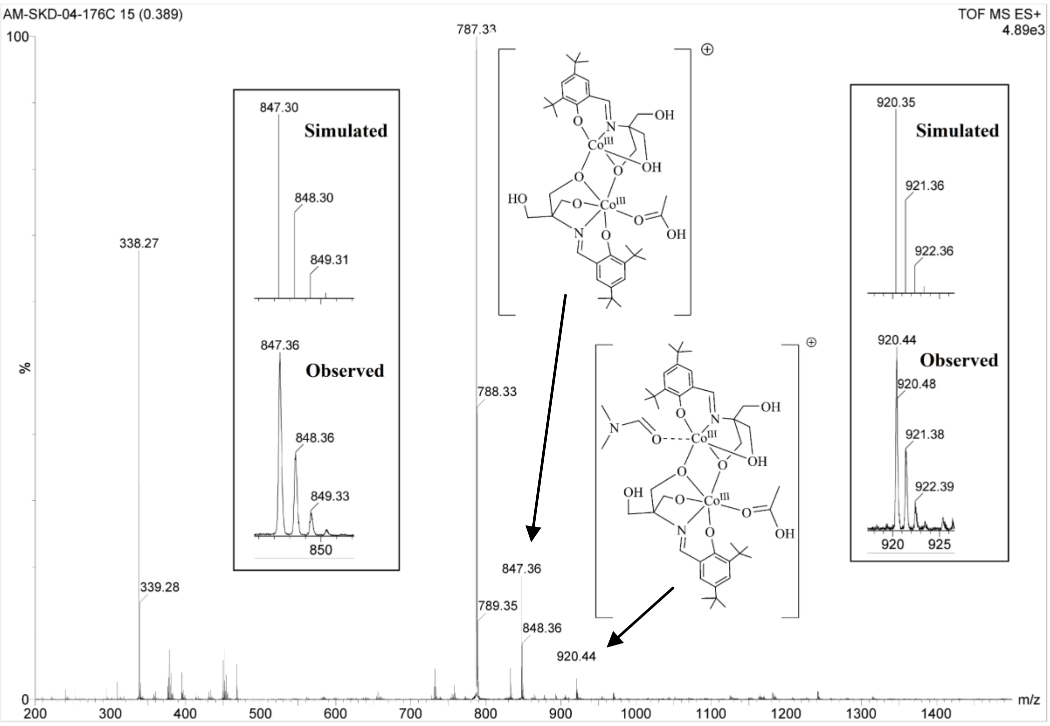

Fig. S20 ESI-MS (+ve ion mode) of the mixture of tetrachlorocatechol (TCC) with complex **1** in (1:1) methanol, acetonitrile mixture with 1% DMF. Reaction condition: 10 μM catalyst (**1**) in air with 500 molar equivalents of TCC. Insets show isotropic distribution of the assigned peaks.

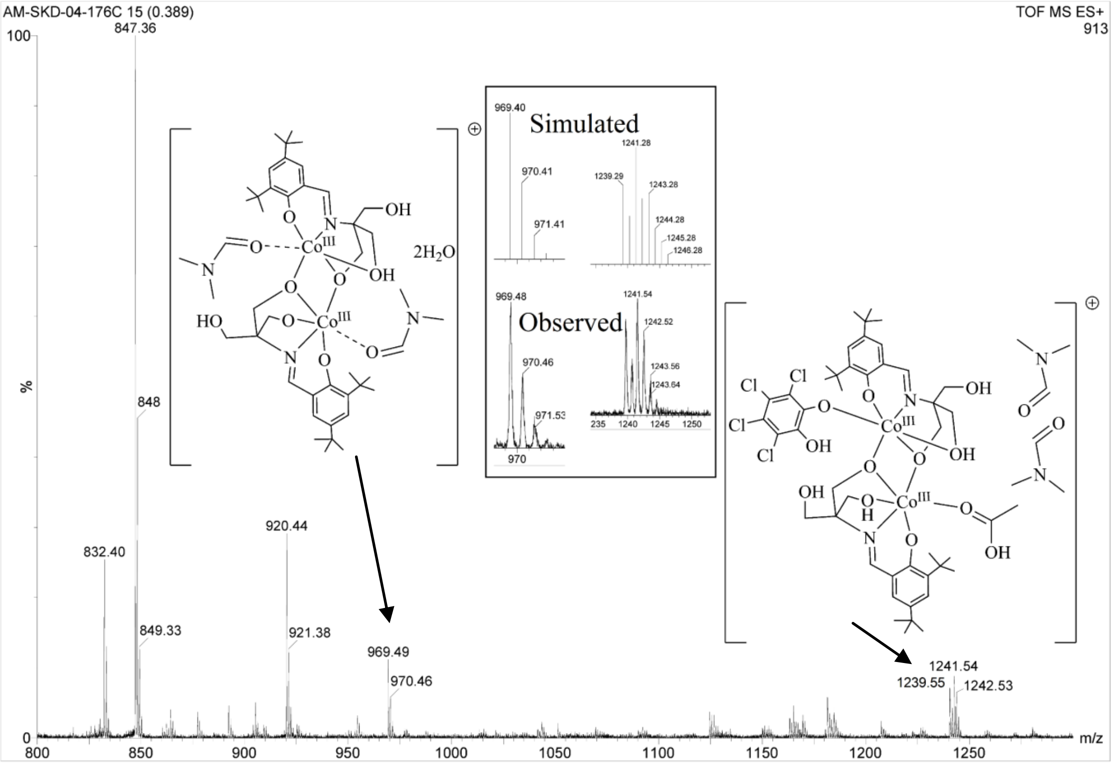

Fig. S21 ESI-MS (+ve ion mode) of the mixture of tetrachlorocatechol(TCC) with complex 1 in (1:1) methanol, acetonitrile mixture with 1% DMF. Reaction condition: 10 μM catalyst (1) in air with 500 molar equivalents of TCC (showing m/z from 800 to 1300). Inset shows isotropic distribution of the assigned peaks.

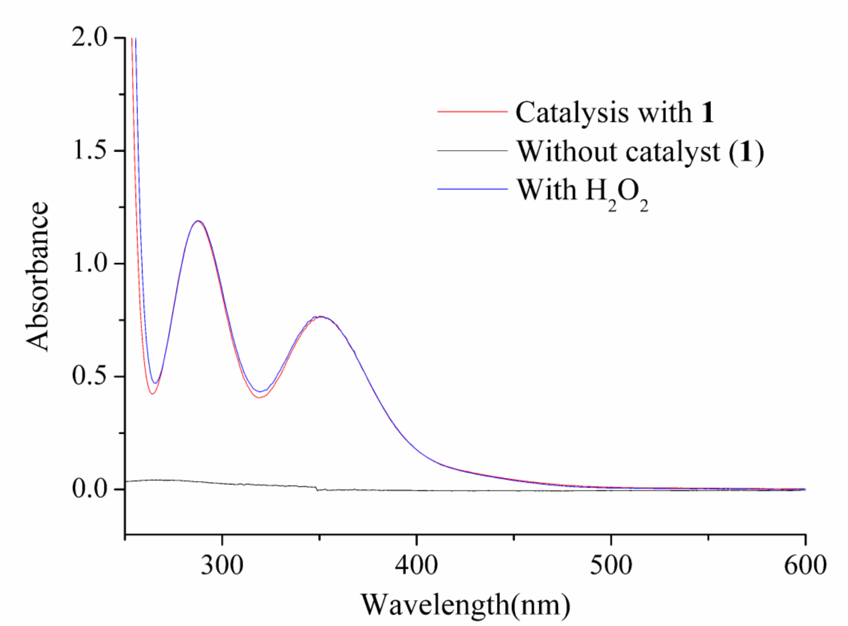

Fig. S22 UV-Vis spectra of hydrogen peroxide detection test showing characteristic peak of I_3^- after DTBC oxidation with catalyst **1.**

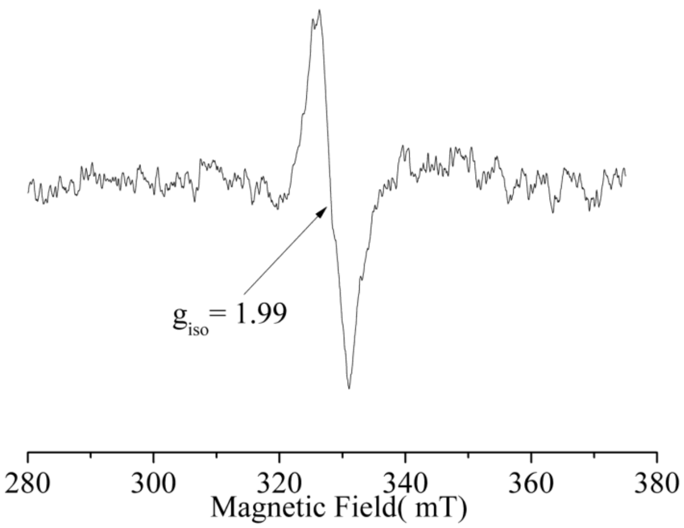

Fig. S23 EPR spectrum of acetonitrile, DMF 9:1 v/v mixture of **1** after addition of 500 equivalent of DTBC, recorded at 77K.

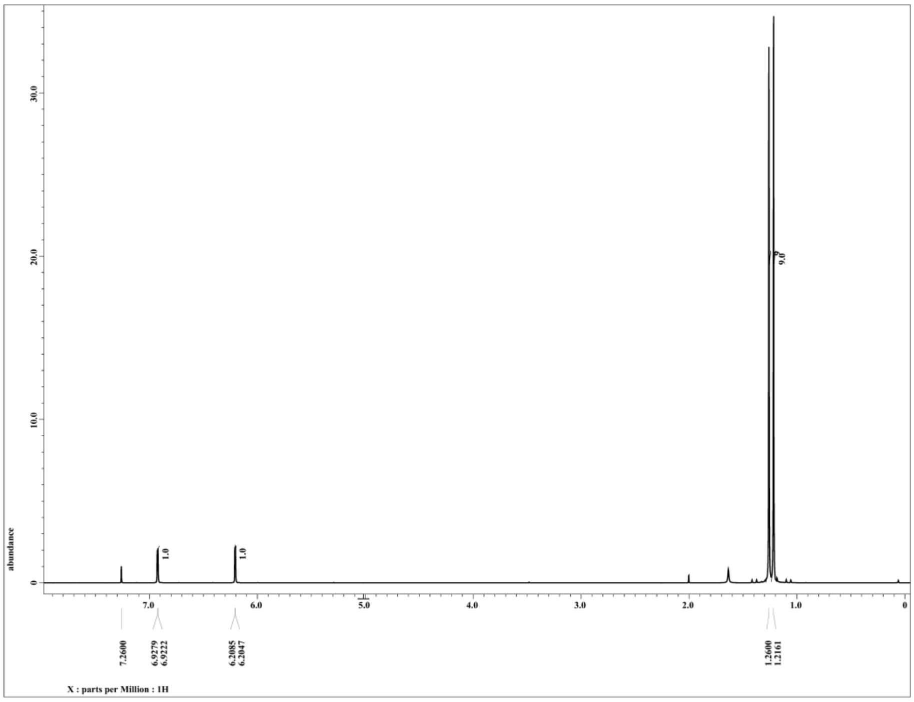

Fig. S24 ^{1}H NMR of DTBQ using $CDCl_3$.

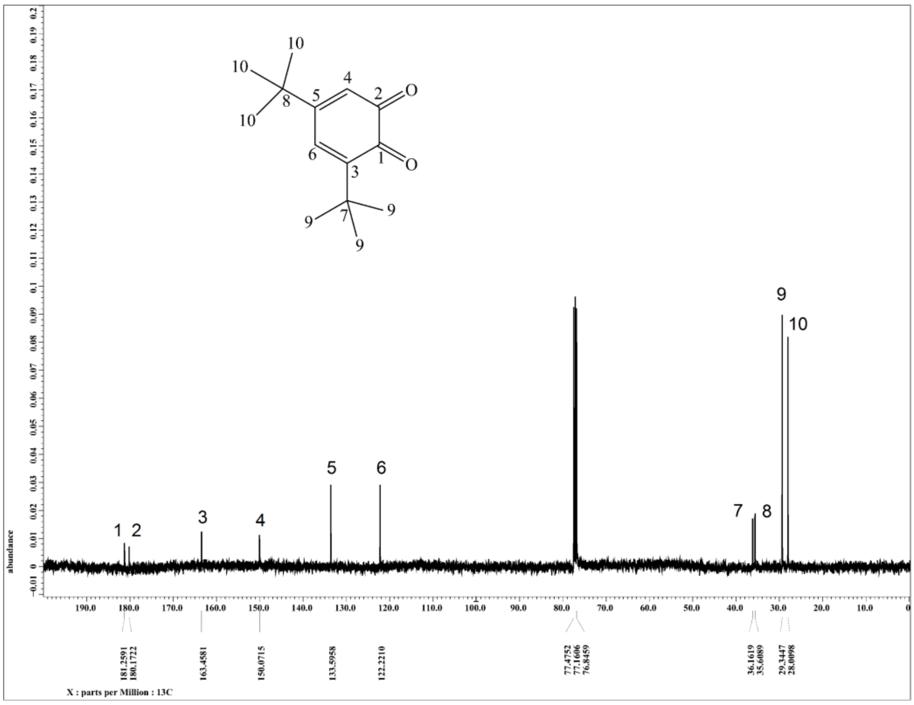

Fig. S25 ^{13}C NMR of DTBQ using $CDCl_3$.